ENVIRONMENTAL RESEARCH
LETTERS

LETTER • OPEN ACCESS

Interplay between climate and carbon cycle feedbacks could substantially enhance future warming

To cite this article: Christine Kaufhold *et al* 2025 *Environ. Res. Lett.* **20** 044027

ENVIRONMENTAL RESEARCH
LETTERS

CrossMark

OPEN ACCESS

RECEIVED
29 July 2024

REVISED
24 January 2025

ACCEPTED FOR PUBLICATION
17 February 2025

PUBLISHED
24 March 2025

LETTER

Interplay between climate and carbon cycle feedbacks could substantially enhance future warming

Christine Kaufhold[1,2,*], **Matteo Willeit**[1], **Stefanie Talento**[1], **Andrey Ganopolski**[1] and **Johan Rockström**[1,3,4]

[1] Potsdam Institute for Climate Impact Research (PIK), Member of the Leibniz Association, PO Box 6012 03, D-14412 Potsdam, Germany
[2] Institute of Physics and Astronomy, University of Potsdam, 14476 Potsdam, Germany
[3] Stockholm Resilience Centre, Stockholm University, SE 106 91 Stockholm, Sweden
[4] Institute for Environmental Science and Geography, University of Potsdam, 14476 Potsdam, Germany
[*] Author to whom any correspondence should be addressed.

E-mail: kaufhold@pik-potsdam.de

Keywords: anthropogenic climate change, climate sensitivity, Earth system modeling, emission scenarios, hothouse

Supplementary material for this article is available online

Abstract

In light of uncertainties regarding climate sensitivity and future anthropogenic greenhouse gas emissions, we explore the plausibility of global warming over the next millennium which is significantly higher than what is usually expected. Although efforts to decarbonize the global economy have significantly shifted global anthropogenic emissions away from the most extreme emission scenarios, intermediate emission scenarios are still plausible. Significant warming in these scenarios cannot be ruled out as uncertainties in equilibrium climate sensitivity (ECS) remain very large. Until now, long-term climate change projections and their uncertainties for such scenarios have not been investigated using Earth system models (ESMs) that account for all major carbon cycle feedbacks. Using the fast ESM CLIMBER-X with interactive CO_2 and CH_4 (the latter typically not included in most models), we performed simulations for the next millennium under extended SSP1-2.6, SSP4-3.4 and SSP2-4.5 scenarios. These scenarios are usually associated with peak global warming levels of 1.5 °C, 2 °C and 3 °C, respectively, for an ECS of $\sim$3 °C, considered the best estimate in the latest Intergovernmental Panel on Climate Change (IPCC) report. As ECS values lower or higher than this estimate cannot be ruled out, we emulate a wide range of ECS from 2 °C to 5 °C, defined as the 'very likely' range by the IPCC. Our results show that achieving the Paris Agreement goal of a 2 °C temperature increase is only feasible for low emission scenarios and if ECS is lower than 3.5 °C. With an ECS of 5 °C, peak warming in all considered scenarios more than doubles compared to an ECS of 3 °C. Approximately 50% of this additional warming is attributed to positive climate–carbon cycle feedbacks with comparable contributions from CO_2 and CH_4. The interplay between potentially high ECS and carbon cycle feedbacks could drastically enhance future warming, demonstrating the importance of properly accounting for all major climate feedbacks and associated uncertainties in projecting future climate change.

1. Introduction

Extensive and concerted research efforts have focused on predicting changes in the Earth's climate over the next century, yet comparatively less effort has been devoted to quantifying the long-term implications of the anthropogenic influence on climate (Forster *et al* 2021). Although it has been known since the beginning of the 21st century that anthropogenic emissions will have a very long lifetime (Archer and Brovkin 2008, Archer *et al* 2009b) and can still have repercussions on the timescale of hundreds of thousands of years (Ganopolski *et al* 2016), it is usually expected that the elevated CO_2 concentration will rapidly decrease after the peak and subsequent cessation of anthropogenic emissions, and that global temperature will follow (MacDougall *et al* 2020). Developments toward the decarbonization of the economy have caused global anthropogenic CO_2 emissions to significantly deviate from the most extreme emission scenarios (e.g. SSP3-7.0 and SSP5-8.5, figure S5) and instead track closer to the lower end of Intergovernmental Panel on Climate Change (IPCC) scenarios (Burgess *et al* 2020), with a plateau and eventual decrease in global emissions forecasted to come (International Energy Agency 2023). These high emission scenarios, developed less than a decade ago and still used for future climate projections today, are becoming increasingly unlikely to represent the future (Hausfather and Peters 2020), whereas medium emission scenarios like SSP2-4.5 still cannot be ruled out (Pielke *et al* 2022). Nevertheless, Steffen *et al* (2018) recently suggested that even modest anthropogenic emissions could cause the destabilization of the Earth's climate through a chain of strongly nonlinear positive feedbacks, pushing it towards a much warmer climate state named 'hothouse'. The possibility that temperature increases from pre-industrial levels could be much higher than usually expected, even in low-to-intermediate emission scenarios, is understudied (Kemp *et al* 2022).

Although some modelling studies have examined the impact of equilibrium climate sensitivity (ECS; Flynn and Mauritsen 2020, Huusko *et al* 2021) and climate–carbon cycle feedbacks (Booth *et al* 2017, Arora *et al* 2020, Melnikova *et al* 2021, Asaadi *et al* 2024) on climate projections, few have focused on systematically examining the climate evolution beyond 2100 CE (Mikolajewicz *et al* 2007, Solomon *et al* 2009, Gillett *et al* 2011). This scarcity is largely due to the high computational costs of Earth system models (ESMs), which have otherwise disregarded or simplified long-term processes (i.e. marine sediment dynamics and chemical rock weathering) that are marginally significant for centennial timescales. Instead, ESMs prioritize short-term processes which are important for the centennial time scales targeted by the IPCC. There are a few notable exceptions, such as permafrost carbon, which are incorporated in only a few ESMs and could crucial for understanding the projected multi-centennial evolution of atmospheric CO_2 concentration. As only a few ESMs have the ability to simulate CH_4 interactively, the long-term impacts of potentially significant carbon cycle feedbacks from permafrost or wetlands have not been accounted for. Previously, Koven *et al* (2022) conducted a multi-model investigation for temperature changes until 2300 CE with prescribed greenhouse gas (GHG) concentrations from selected shared socioeconomic pathway (SSP) scenarios. Zickfeld *et al* (2013) also performed a multi-model investigation over the next millennium, and found temperature changes at 3000 CE of $\sim-0.2\,^{\circ}$C–0.7 °C for RCP2.6, and $\sim$1.3 °C–2.3 °C for RCP4.5 in simulations with interactive CO_2 concentration but prescribed CH_4. However, most models in Zickfeld *et al* (2013) have ECSs close to 3 °C and extremely high temperature changes ($\gtrsim$6 °C) were only seen in experiments with large anthropogenic emissions.

The uncertainties in anthropogenic climate change predictions primarily originate from future emission scenarios and climate sensitivity. The latter is determined by the strength of several climate feedbacks, some of which, especially the cloud feedback, are rather uncertain (Schneider *et al* 2019, Mann 2021). It is for this reason constraining the Earth's ECS, defined as the steady-state global-mean surface air temperature change due to a doubling atmospheric CO_2, is considered to be of fundamental importance for climate science (Sherwood and Forest 2024). Observational data only provides loose constraints on ECS given the limited time period of instrumental observations that is further complicated by the many uncertainties in anthropogenic radiative forcing (Carslaw *et al* 2013, Lee *et al* 2016, Gregory *et al* 2020). Attempts at constraining the ECS using paleoclimatic data have also been performed (Rohling *et al* 2012), but this approach has limitations as the most comprehensive data available originates from cold (i.e. glacial) conditions. Since ECS can be strongly climate-dependent (Pfister and Stocker 2017, Bloch-Johnson *et al* 2021), climate sensitivity derived from colder climates is not necessarily applicable to warmer climates. Understanding how feedback processes operate in warm climatic conditions (Caballero and Huber 2013, Shaffer *et al* 2016), as well as any emergent constraints on ECS (Caldwell *et al* 2018), are still in the early stages of investigation.

State-of-the-art ESMs and climate models which participated in the Coupled Model Intercomparison Project Phase 6 (CMIP6) exhibit a large spread in ECS (1.8 °C–5.6 °C, Forster *et al* 2021), with ten models reportedly having an ECS larger than 4.5 °C (Zelinka *et al* 2020). This wide range in ECS estimates is primarily attributed to the different strengths of climate feedbacks, with cloud feedbacks exhibiting the largest uncertainty (Zelinka *et al* 2020). Although the IPCC estimates the 'very likely' range of ECS is 2 °C–5 °C (with a best estimate of 3 °C, Forster *et al* (2021)), values even higher than 5 °C cannot be disregarded as impossible at the present time (Knutti *et al* 2017, Bjordal *et al* 2020, Rugenstein *et al* 2020, Sherwood *et al* 2020, Mann 2021, Wall *et al* 2022). While there is a tendency for CMIP6 models with high ECS to overestimate the historical warming trend, at least some models with very different ECS can skillfully represent the increase of the global-mean surface temperature over the industrial era (Nijsse *et al* 2020, Tokarska *et al* 2020). This can be at least partly explained by the stronger negative aerosol forcing offsetting the impact of high ECS in these models (Meehl *et al* 2020), as the direct and indirect effects of aerosols on the radiation balance and clouds are very uncertain (Lohmann *et al* 2010, Myhre *et al* 2013, Zelinka *et al* 2013, Wall *et al* 2022).

Recent studies suggest that the likelihood of ECS to be above 4.5 °C (the former upper bound of the IPCC range) is approximately 10%, and 5% for ECS above 5 °C (Sherwood *et al* 2020). While these high ECS values are by no means very likely, they cannot be entirely ruled out, and comprehensive risk management still demands an assessment of even the most extreme cases, regardless of the likelihood (Kemp *et al* 2022, Davidson and Kemp 2024). Investigating uncertainties related to climate sensitivity, feedbacks in the carbon cycle, and tipping points under more realistic scenarios are, therefore, more pertinent, especially as high emission pathways like SSP3-7.0 and SSP5-8.5 are becoming less aligned with current emission trends (Burgess *et al* 2020, Hausfather and Peters 2020, Pielke *et al* 2022, Hausfather 2025). In this study, we investigate the effect of carbon cycle feedbacks and uncertainties in climate sensitivity on global warming using the newly developed ESM CLIMBER-X (Willeit *et al* 2022, 2023). We perform millennium-long simulations of the future climate under three low-to-intermediate GHG emission scenarios as defined by the SSPs emulating different ECS in the range of 2 °C–5 °C (Forster *et al* 2021). This approach provides insights into plausible future climate trajectories, and demonstrates that the combined effect of fast and slow positive climate feedbacks can induce significant temperature changes, even under relatively low anthropogenic emission scenarios.

2. Methods

2.1. ESM

CLIMBER-X (Willeit *et al* 2022, 2023, 2024) is a fast ESM which was specifically designed to simulate the evolution of the Earth system on timescales ranging from decades to hundreds of thousands of years. It is computationally efficient, which allows CLIMBER-X to perform the large number of long simulations which are required to explore the response of the Earth system to anthropogenic forcing over the current millennium. This is also possible because processes related to synoptic/interannual variability and diurnal cycles are not explicitly represented. The model has a horizontal resolution of $5^\circ \times 5^\circ$ and uses a daily time-step. The comprehensive evaluation of model performance conducted by Willeit *et al* (2022) includes an assessment for both climate of the present-day and for the historical period. Not only does this evaluation involve model-data comparisons to assess accuracy in simulating past conditions, but it also provides model-model comparisons for climate feedbacks and future climate projections. Willeit *et al* (2023) shows that CLIMBER-X well reproduces historical CO_2 and CH_4 changes, as well as carbon cycle feedbacks and sensitivities, and its performance is generally comparable to state-of-the-art ESMs.

The climate component of CLIMBER-X is described in detail in Willeit *et al* (2022), while the details of the global carbon cycle model are presented in Willeit *et al* (2023). Of particular relevance for this study is that CLIMBER-X includes a fully interactive carbon cycle, which enables it to interactively compute the evolution of atmospheric CO_2 and CH_4 concentrations for given emission scenarios, therefore explicitly taking into account the carbon cycle feedbacks. The comprehensive carbon cycle model includes the explicit treatment of permafrost carbon, chemical rock weathering and natural methane emissions from wetlands. Although CLIMBER-X has the capability to simulate ice sheets interactively (Willeit *et al* 2024), they are prescribed by their present-day state in model simulations presented in this study to maintain a more straight-forward analysis between climate and carbon cycle feedbacks.

2.2. Ensemble with different climate sensitivities

Climate models exhibit a wide range of ECS values, contributing to significant uncertainties in future climate projections when combined with different anthropogenic emission scenarios. Comparing results of climate model simulations carried out within CMIP6 is a direct way to assess these uncertainties, but for SSP1-2.6 and SSP2-4.5, simulations generally only extend to 2100 and use prescribed GHGs, limiting investigations on the interplay between ECS and climate–carbon cycle feedbacks. An alternative approach involves creating a perturbed physics ensemble within a single model (Murphy *et al* 2004), but this method addresses only parameter uncertainties and lacks the structural uncertainties of multi-model ensembles (Yamazaki *et al* 2021). Moreover, most members of such an ensemble simulate the present climate much less realistically than the properly calibrated original model version (Schneider von Deimling *et al* 2006).

To overcome these limitations, we use a scaling method to adjust GHG radiative forcing, enabling emulation of different ECSs within a single model without compromising the pre-industrial state. Climate sensitivity in the standard CLIMBER-X model version is ∼3 °C (Willeit *et al* 2022). This model configuration is used in the reference experiments, however, we additionally create a model ensemble which emulates a spectrum of different ECS values ranging from 2 °C–5 °C (given as the 'very likely' range in the latest IPCC report, Forster *et al*

2021). Unlike conventional approaches to exploring the uncertainty of ECS by modifying the strength of individual climate feedbacks, here we instead scale the radiative forcing of GHGs as follows:

$$CO_2^{eq,\alpha} = e^{\left(\alpha \ln CO_2^{eq} + (1-\alpha)\ln CO_2^{ref}\right)} \quad (1)$$

where α is the scaling coefficient ($\alpha = \frac{ECS}{ECS_0}$), ECS is the is the ECS we want to emulate, $ECS_0 = 3\,^\circ C$ is the standard ECS of CLIMBER-X, $CO_2^{ref} = 280$ ppm is the reference pre-industrial CO_2 concentration and CO_2^{eq} is the equivalent CO_2 concentration for radiation, which includes also the effect of the other GHGs (i.e. CH_4, N_2O and CFCs) as described in Willeit *et al* (2022). By definition, ECS excludes feedbacks from the carbon cycle, and primarily accounts for fast climate feedbacks such as those from water vapor, lapse rate, clouds, and albedo. The scaling method introduced here only affects the CO_2 concentration used in the radiation scheme, but does not directly influence the actual CO_2 simulated as part of the carbon cycle in CLIMBER-X. Although the radiative forcing of GHGs also has some uncertainties, the main source of uncertainty in the ECS is the climate feedbacks, primarily the cloud feedback. Thus, our scaling approach is based on a strong assumption that the response of climate models with different ECS to radiative forcing can be mimicked by scaling the forcing rather than changing the model physics. Validation confirms that this method reproduces the results of models with different ECSs (see SI), including global and spatial temperature patterns as simulated by CMIP6 models with different ECSs (figures S3, S11, S12 and S13); critical for the representation of climate–carbon cycle feedbacks. Simple ways of scaling ECS have been applied in previous studies (Govindasamy *et al* 2005, Colbourn *et al* 2015, Clark *et al* 2016, Tanaka and O'Neill 2018, Bouttes *et al* 2024).

2.3. Experimental set-up

All model simulations are initialized from a pre-industrial equilibrium state that is obtained from a 100 000 year equilibrium spinup procedure as described in Willeit *et al* (2023). Since the ECS scaling procedure and the aerosol forcing do not affect the pre-industrial climate, the pre-industrial equilibrium state is the same for all ensemble members with different ECS. For the historical period we apply standard forcings used also in the CMIP6 model simulations, as described in Willeit *et al* (2022) and Willeit *et al* (2023). Since our model simulations are emission driven (for both CO_2 and CH_4), anthropogenic CO_2 and CH_4 emissions are prescribed instead of concentrations. For the future projections we apply the extended SSP1-2.6, SSP4-3.4 and SSP2-4.5 scenarios as CO_2 emissions have been tracking reasonably close to all three since 2015 (Meinshausen *et al* 2020, figure S5). This is more extensively described in the SI (section S1.3).

3. Results

3.1. Future climate change in the reference simulation

Figure 1 shows global air temperature, atmospheric CO_2 and CH_4 concentrations and steric sea level rise over the whole simulated period (1850–3000 CE), across different model versions and three SSP scenarios. All model versions with different climate sensitivity not only realistically reproduce historical changes in global temperature, but also atmospheric concentration of CO_2 and CH_4 (figure 1). The results of the reference simulation with ECS = 3 °C is described next, while the effect of the uncertainties in ECS is explored in section 3.2. The simulated atmospheric CO_2 concentration in our reference runs (ECS = 3 °C) closely follows the scenarios of Meinshausen *et al* (2020). All simulations exhibit a rapid increase of atmospheric CO_2 concentration, which is largely controlled by the prescribed SSP scenario (figure S2(a)). Peak CO_2 concentration generally occurs around 2060 CE for SSP1-2.6, 2085 CE for SSP4-3.4, and 2220 CE for SSP2-4.5 (figures 1(d)–(f)). In our reference runs, peak CO_2 concentrations are approximately 470, 500 and 640 ppm for SSP1-2.6, SSP4-3.4 and SSP2-4.5, respectively. By 2500 CE, small differences relative to Meinshausen *et al* (2020) become apparent as our simulations indicate a more significant decline in CO_2 concentrations. The CH_4 concentration in our reference run falls in between that of previous studies (Meinshausen *et al* 2020, Kleinen *et al* 2021), with peak concentrations in the SSP1-2.6, SSP4-3.4 and SSP2-4.5 scenarios of approximately 1990, 2400 and 2200 ppb. In SSP1-2.6 and SSP2-4.5, the model simulates higher atmospheric CH_4 levels than Meinshausen *et al* (2020) because we not only account for anthropogenic CH_4 emissions, but also increases in natural emissions from wetlands as a response to increasing vegetation productivity and rising soil temperatures. These factors have been shown to substantially increase natural CH_4 emissions and consequently atmospheric CH_4 levels (Kleinen *et al* 2021). Our simulated CH_4 concentrations are lower than those in Kleinen *et al* (2021) (figures 1(g) and (i)). This is mainly because we make the conservative assumption that the atmospheric lifetime of CH_4 is constant, although it has been shown it is generally increasing in the long-term under global warming (Lelieveld *et al* 1998, John *et al* 2012, Voulgarakis *et al* 2013). In SSP4-3.4, the CH_4 concentration in Meinshausen *et al* (2020) is quite similar to our reference because anthropogenic CH_4 emissions dominate over natural emissions in this scenario (figures S2(b) and S6(b)).

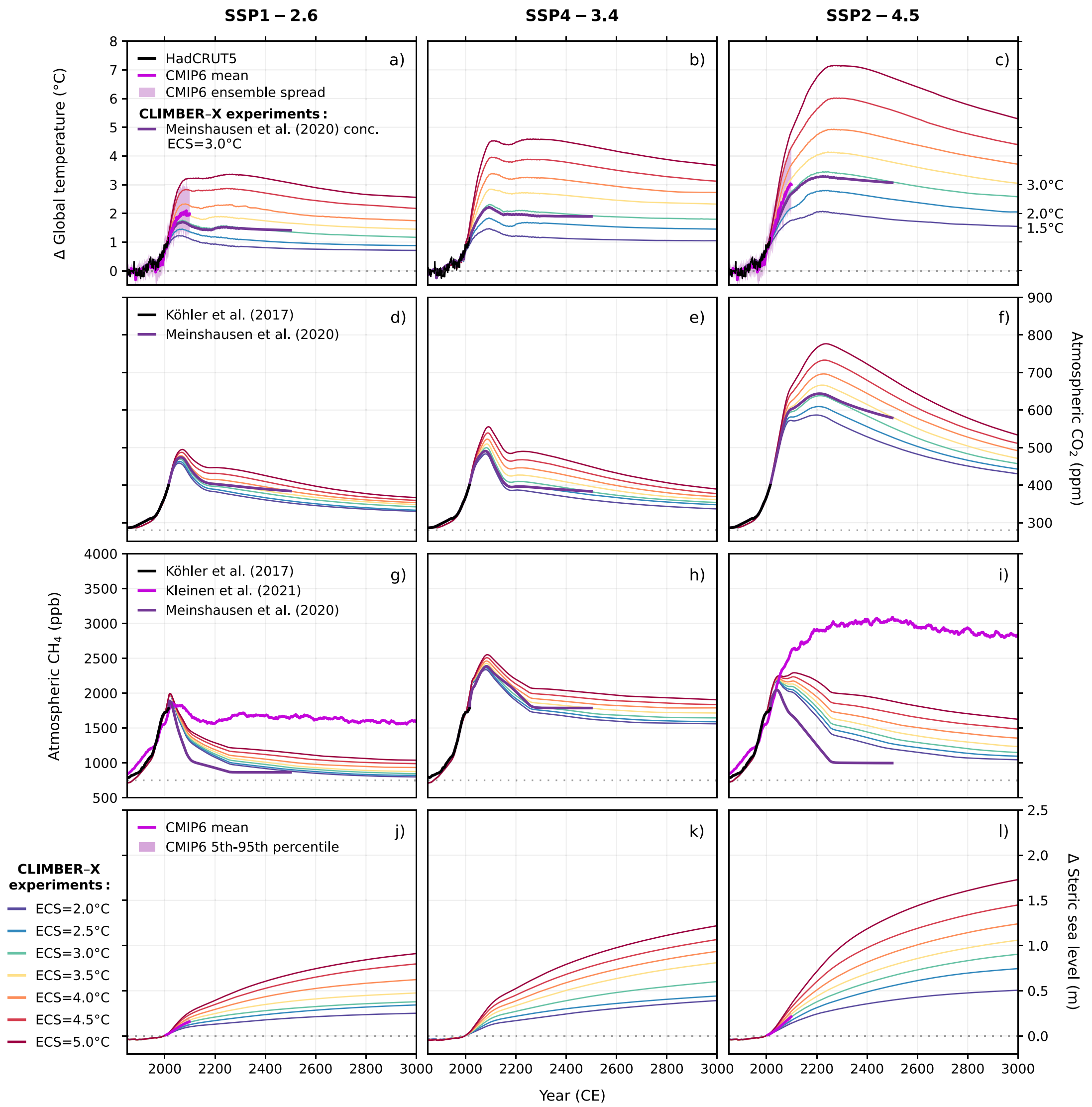

Figure 1. Global changes in (a)–(c) surface air temperature, (d)–(f) atmospheric CO_2 concentration, (g)–(i) CH_4 concentration, and (j)–(l) steric sea level from 1850–3000 CE, following the SSP1-2.6, SSP4-3.4 and SSP2-4.5 scenarios. Global mean temperature has been taken relative to 1850–1880 CE, and global mean thermal expansion is relative to 1986–2005 CE. The colors represent simulations with interactive CO_2 and CH_4 under different ECS values. Observational values (Köhler *et al* 2017, Morice *et al* 2021) are provided in black, whereas any comparable studies (Meinshausen *et al* 2020, Hermans *et al* 2021, Kleinen *et al* 2021) have been provided in assorted shades of purple. Simulated temperature changes for a set of CLIMBER-X experiments has also been plotted in (a) and (b) using prescribed concentrations from Meinshausen *et al* (2020). CMIP6 data for global mean temperature has been smoothed with a 30 year running mean to remove interannual variability.

Under future SSP scenarios (figure S2), temperatures continue to rise following the increase in atmospheric CO_2 and CH_4 concentrations. While SSP1-2.6, SSP4-3.4 and SSP2-4.5 are often associated with 1.5 °C, 2 °C and 3 °C of warming, we see peak values of approximately 1.8 °C, 2.3 °C, 3.5 °C in our reference run (ECS = 3 °C, figures 1(a)–(c)). Once anthropogenic CO_2 emissions are no longer supplied to the atmosphere, the atmospheric burden starts to diminish as carbon continues to be taken up by the ocean (figures 2(d)–(f)). In turn, we observe that global mean temperature begins to decline over the next millennium. Under the reference ECS, temperatures at the year 3000 CE are still 1.2 °C, 1.8 °C, 2.6 °C higher than pre-industrial levels in the SSP1-2.6, SSP4-3.4 and SSP2-4.5 scenarios.

The high-latitudes consistently show the largest changes in temperature (figure 3). At 2300 CE, warming in the SSP1-2.6 and SSP4-3.4 scenarios is particularly pronounced over areas of the Arctic Ocean with retreating sea ice margins, like that of the Greenland and Barents-Kara seas (figures 3(a) and (b)). Arctic temperatures in SSP1-2.6 exhibit an average increase of approximately 4 °C by year 2300, which can reach up to 11 °C in some regions (figure 3(a)). In SSP2-4.5, the average temperature in the Arctic nearly doubles

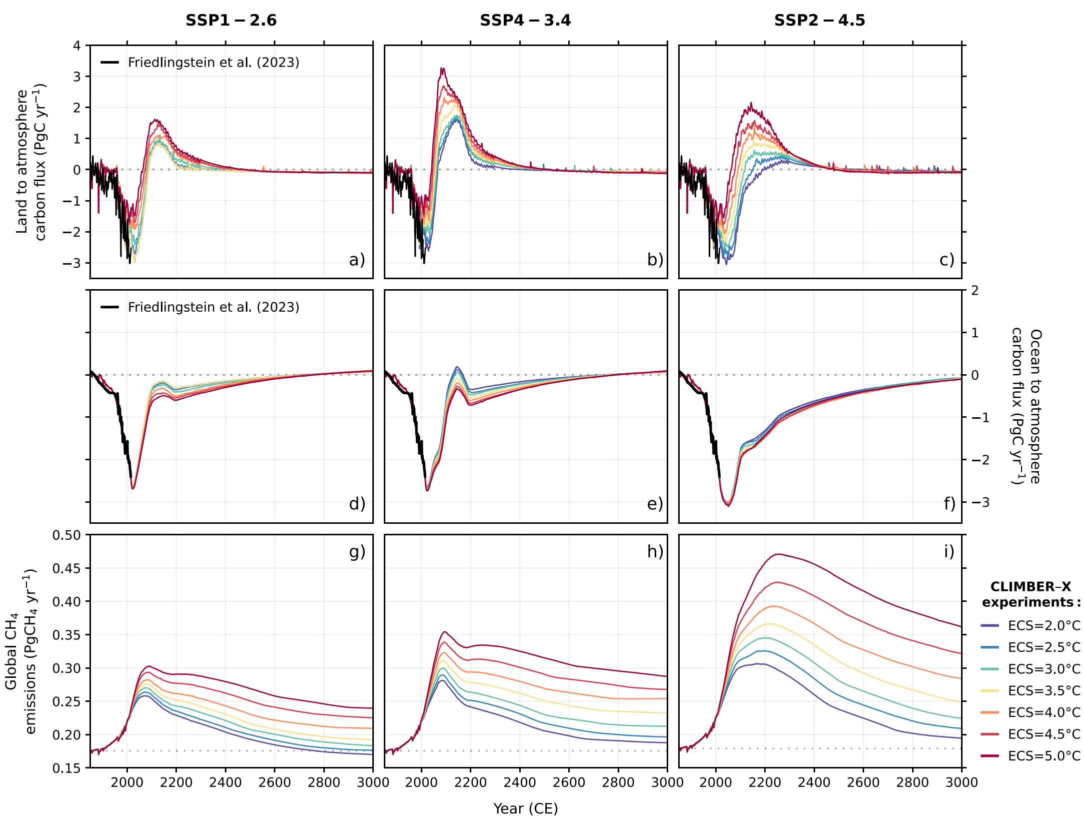

Figure 2. Carbon fluxes of (a)–(c) the land to atmosphere, (d)–(f) ocean to atmosphere, and (g)–(i) global natural methane emissions over the entire simulated period (1850–3000) and across the different SSP scenarios. Positive values represent carbon flux to the atmosphere. Observational data (Friedlingstein *et al* 2023) has been provided in the black line, and experiments under different ECS values is given by the colored line. Land to atmosphere carbon flux was plotted with a 3 year moving average for visibility.

compared to SSP1-2.6, with some regions having temperature increases up to ∼15 °C by 2300 CE (figures 3(c) and (j)). The increased warming of the high-latitudes is primarily attributed to polar amplification, caused by the reduction of sea ice and snow (surface-albedo feedback) and surface confinement of warming (positive lapse-rate feedback). While summer sea ice area at 2300 CE ranges between 1–2 million km^2 in the SSP1-2.6 and SSP4-3.4 scenarios, this value approaches near-zero in SSP2-4.5 (figures S7(a)–(c)). Winter sea ice also decreases substantially (figures S7(a)–(c)). Permafrost area decreases between ∼30%–60% compared to the pre-industrial, depending on the emission scenario (figures 3(d)–(f)) and S8(a)–(c)). The spatial patterns of temperature change at the time of peak global warming closely resemble those at the end of the millennium (figures 3(d)–(f)).

Steric sea level rise, primarily caused by the thermal expansion of sea water, continues to increase across all SSP scenarios long after emissions cease (figures 1(j)–(l)). Like CO_2 concentration, steric sea level in our reference scenario follows the CMIP6 mean over the current century quite closely (figures 1(j) and (l)). In SSP1-2.6, sea level increases by approximately 0.4 m by the end of the millennium from thermosteric changes alone. This value increases with larger cumulative emissions, as steric sea level rises by 0.9 m in SSP2-4.5 at the year 3000. We note that thermosteric changes under the reference sensitivity generally agree with magnitudes reported by previous studies: Zickfeld *et al* (2013) found an ensemble mean of 0.4 m and 0.8 m for RCP 2.6 and RCP 4.5 at the year 3000.

3.2. Impact of climate sensitivity on future climate change

Uncertainties in climate sensitivity cause a substantial spread in the simulated temperature change (figures 1(a)–(c)). A similar uncertainty range is produced by the CMIP6 ensemble, mainly due to the large spread in ECS among CMIP6 models (table S1). In the case when we used the same forcings as in CMIP6, the results for SSP1-2.6 and SSP2-4.5 are in good agreement with CMIP6 models (figures S3(a) and (b)). However, in simulations with the interactive carbon cycle (figures 1(a) and (c)), our highest simulated temperature change exceeds the range of

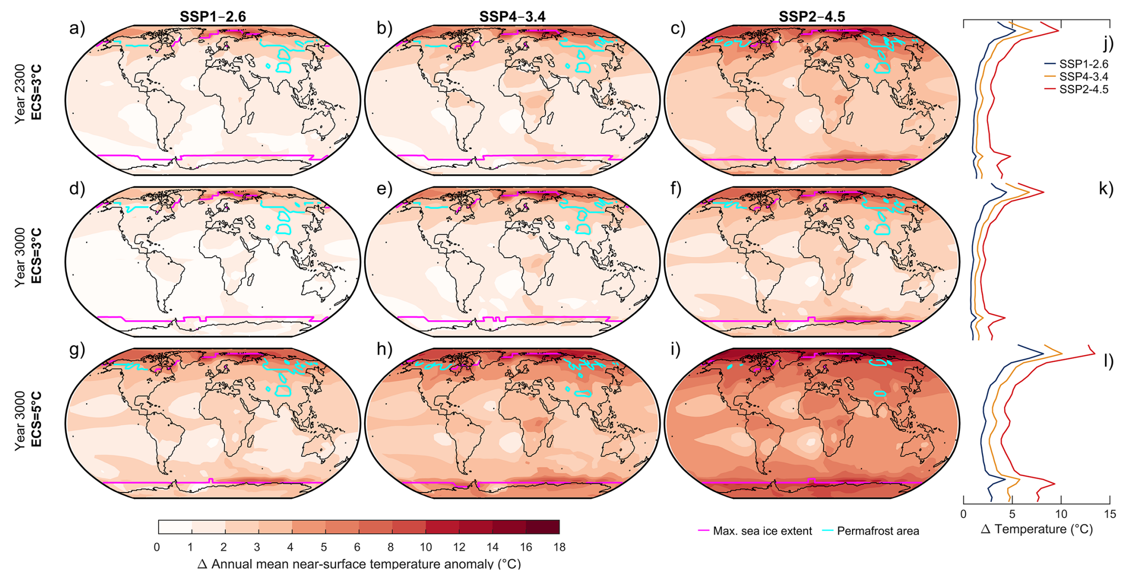

Figure 3. Changes in annual mean near surface air temperature at selected timeslices relative to the pre-industrial period under the SSP1-2.6, SSP4-3.4 and SSP2-4.5 emisson scenarios and different ECS conditions. (a)–(c) Peak warming around year 2300 CE, (d)–(i) remaining temperature increase by the end of the current millennium for (a)–(f) ECS = 3 °C and (g)–(i) ECS = 5 °C. Magenta lines (a)–(i) display the annual maximum sea ice extent, whereas cyan lines (a)–(i) display the permafrost area. Zonal mean temperature changes (j)–(l) are additionally shown for SSP1-2.6 (blue), SSP4-3.4 (yellow), and SSP2-4.5 (red) across the rows. Contour intervals and colorbar are nonlinear as to provide visual clarity of small temperature changes.

CMIP6 models, even though the highest ECS considered in our experiments (5 °C) is lower than the maximum ECS in the CMIP6 ensemble (5.6 °C). This is related to the positive carbon cycle feedbacks in our model. High ECS values are associated with greater warming and larger CO_2 and CH_4 concentrations than in the reference run, with the reverse being true for low ECS values. In addition to this, the spread in temperature due to different ECS generally increases with increasing cumulative emissions. Compared to the reference run, low climate sensitivity (ECS = 2 °C) results in global temperature anomalies which are approximately 0.5 °C, 0.8 °C and 1.4 °C lower, corresponding to temperature peaks of just 1.2 °C, 1.5 °C and 2.1 °C across the different emission scenarios. On the contrary, a high ECS (ECS = 5 °C) can cause additional temperature increases of approximately 1.6 °C, 2.3 °C and 3.7 °C in the SSP1-2.6, SSP4-3.4, and SSP2-4.5 scenarios compared to the reference run, leading to maximum global mean temperature anomalies of around 3.4 °C, 4.6 °C and 7.2 °C; roughly twice the maximum warming produced with ECS = 3 °C. Therefore, there is a non-negligible probability that, despite the ambitious decarbonization efforts in SSP1-2.6, Earth can undergo ∼3.5 °C warming (figure 1(a)). This possibility increases to 10% for ECS = 4.5 °C (Sherwood *et al* 2020), which anticipates a ∼3 °C peak increase in our simulations (figure 1(a)). According to our simulations, achieving the goal of a 1.5 °C temperature increase as outlined in the 2015 Paris Agreement (UNFCC 2015) is only feasible for SSP1-2.6 if ECS is lower than the current best estimate of 3 °C (Forster *et al* 2021). This implies that, if ECS is greater than 3 °C, carbon reduction and removal must be even faster than the SSP1-2.6 scenario to 'keep 1.5 °C alive'.

Climate sensitivity also has a sizeable effect on temperatures simulated at the end of the millennium, with projected warming at 3000 CE ranging from 0.7 °C–1.5 °C when ECS = 2 °C, to 2.6 °C–5.3 °C when ECS = 5 °C, depending on the scenario. Increasing ECS from the reference 3 °C to 5 °C results in a significant rise in temperatures worldwide, resulting in larger differences compared to the pre-industrial (figures 3(g)–(i)). Temperature increases in the Arctic more than double when compared to the global mean under all emission scenarios (figure 3(l)).

Atmospheric CO_2 concentration in the SSP scenarios is higher by 26–138 ppm for a high ECS, and lower by 11–52 ppm for a low ECS, compared to the reference run. Similar differences are seen in CH_4 concentration but in ppb. By the end of the millennium, sea level rise from thermosteric changes is highly dependent on ECS, and ranges from ∼0.3–0.9 m in SSP1-2.6, to ∼0.5–1.7 m in SSP2-4.5.

3.3. Role of carbon cycle feedbacks

The simulated additional global warming under high ECS is disproportionately larger than what is expected from a simple linear relation between climate sensitivity and global warming. For instance, an increase of ECS from 3 °C to 5 °C (factor 1.66 increase) leads

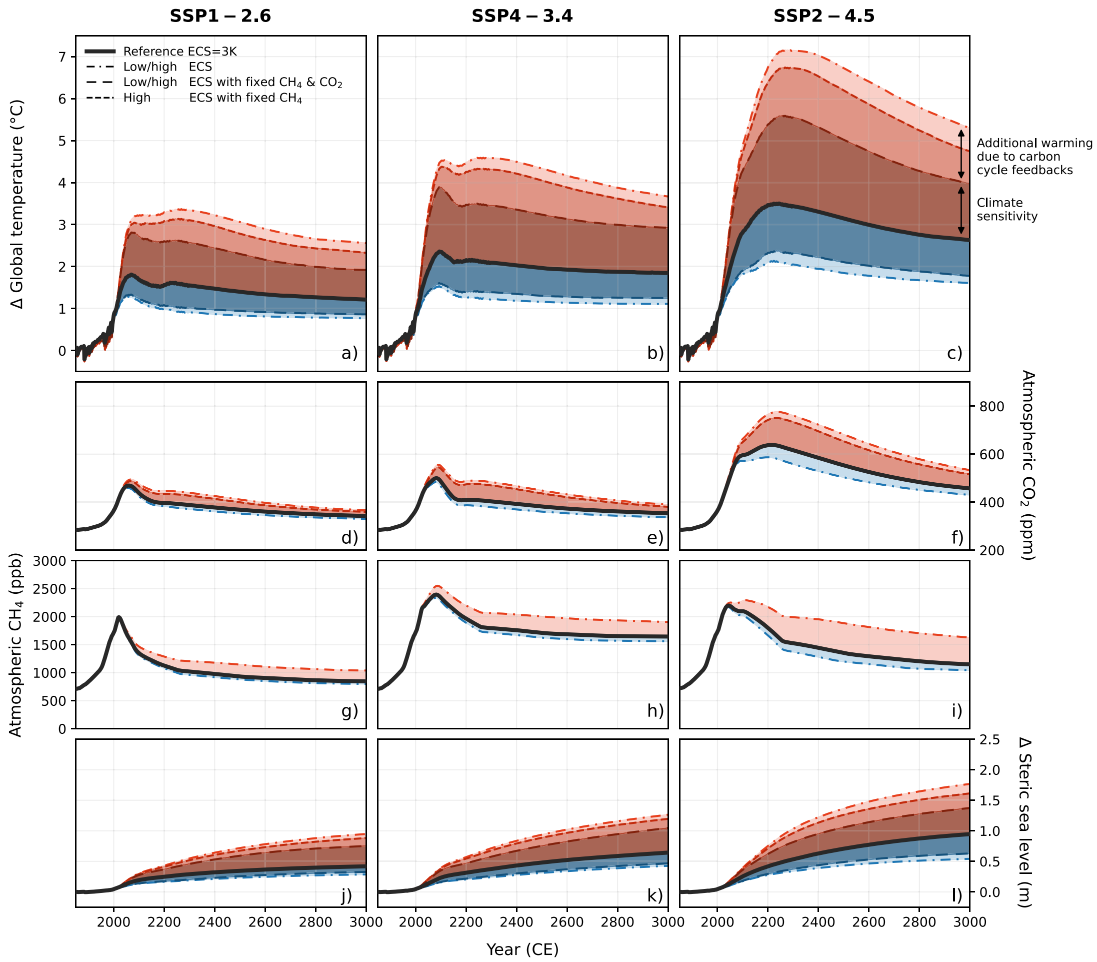

Figure 4. Attribution of changes in (a)–(c) global mean temperature, (d)–(f) CO_2 concentration, (g)–(i) CH_4 concentration, and (j)–(l) steric sea level resulting from climate sensitivity and additional carbon cycle feedbacks. Here, we use ECS = 5 °C for the high ECS considered, and ECS = 2 °C for the low ECS considered. The trajectories for ECS = 2 °C and 5 °C (in the dotted-and-dashed lines) are equivalent to those plotted in figure 1. For ECS = 5 °C, additional carbon cycle feedbacks can be broken down into contributions from CO_2 (area between dashed and tightly dashed lines), and CH_4 (area between tightly dashed and dotted-and-dashed lines). The warming contribution due to climate–carbon cycle feedbacks in the ECS = 5 °C case is additional warming due to changing climate sensitivity, as compared to the case where ECS = 3 °C. Temperature and steric sea level is relative to 1850–1880 CE.

to a temperature increase by more than a factor of two (figures 1(a)–(c)). This is because a substantial portion of the temperature changes can be attributed to positive carbon cycle feedbacks, which act to increase the atmospheric concentrations of CO_2 and CH_4 (Govindasamy *et al* 2005). By running additional experiments under different ECS values, and prescribing CO_2 and CH_4 concentrations from the reference run, we separated the contribution of the carbon cycle feedbacks to temperature changes (figure 4).

Across the different scenarios, we find that carbon cycle feedbacks as a whole are responsible for nearly half of the additional temperature increase (compared to the reference climate sensitivity) when ECS is high, meaning that this effect is equally as important as the change in climate sensitivity (figures 4(a)–(c)). High climate sensitivity (ECS = 5 °C) is responsible for an additional 0.7 °C, 1.0 °C and 1.3 °C by the end of the millennium compared to the reference run for the SSP1-2.6, SSP4-3.4, and SSP2-4.5 scenarios. Carbon cycle feedbacks additionally increases this temperature by 0.6 °C, 0.7 °C and 1.3 °C (figures 4(a)–(c)). In simulations with a low ECS, however, the effect of carbon cycle feedbacks is not as strong, and the majority of temperature changes come from changes in climate sensitivity. The additional temperature change from carbon cycle feedbacks can be further broken down into contributions from CO_2 and CH_4 (figure 4), with the effect of CO_2 on temperature being larger than that of CH_4 across all SSP scenarios. Accounting for changes in the atmospheric lifetime of CH_4, thereby resulting in simulated CH_4 concentrations closer to those in Kleinen *et al* (2021) (figure 1(c)), would lead to the effects of CO_2 and CH_4 being more similar.

The response of the land carbon cycle to climate changes is primarily controlled by two opposing feedback mechanisms. The first is the CO_2 fertilization effect, which increases land carbon uptake and occurs because higher CO_2 concentrations stimulate vegetation to consume more carbon via photosynthesis (negative land CO_2–carbon cycle feedback). The second, warming-enhanced soil respiration, reduces land carbon uptake and occurs when CO_2 is released from the soil from heightened microbial activity (positive land climate–carbon cycle feedback). The positive carbon cycle feedback as a whole (i.e. including the ocean) is driven mainly by the land carbon response (figures 2(a)–(c)) through the temperature dependence of soil respiration. Different ECS strongly impact the amount of carbon stored in soils, with a larger ECS resulting in less soil carbon (figures S9(g)–(i)), while changes in vegetation carbon are only marginal (figures S9(d)–(f)) and driven by changes in net primary production (figures S9(a)–(c)). In our simulations the positive climate–carbon cycle feedback dominates over the negative CO_2–carbon cycle feedback as ECS increases.

Over the historical period (1850–2015 CE), vegetation carbon decreases due to land use change, while soil carbon increases. This changes during the 21st century as land becomes a net sink of carbon across all emission scenarios (figures 2(a)–(c)) from increases in net primary productivity (figures S9(a)–(c)). This agrees with earlier studies (Brovkin *et al* 2013). While increases in vegetation carbon are largely dependent on the SSP scenario over the 21st century (figures S9(d)–(f)), ECS has a large role in determining the magnitude of these changes. Globally, soil carbon shows an initial increase across the different SSP scenarios, reaching its peak earlier under high ECS values. This is followed by a rapid decrease, which results in the soil carbon reservoir being either a net source (high ECS) or net sink (low ECS), depending on climate sensitivity (figures S9(g)–(i)). A substantial part of the positive land carbon cycle feedback can be attributed to the changes in carbon stored in permafrost. More than 50% (61%–94%) of permafrost area is lost in simulations when ECS $= 5\,^\circ$C (figure S8), where the majority of held carbon is released back into the atmosphere (figures S10(g)–(i)). Although permafrost area decreases in simulations with a low ECS, the corresponding carbon loss in soil is dampened to some degree by an increase in net primary production (figures S10(a)–(c)) and a consequently larger carbon input to the soil. The higher the ECS, the less carbon is stored on land at all times. By the year 3000 CE in SSP1-2.6, the land stores 50 PgC more carbon than at pre-industrial if ECS $= 2\,^\circ$C, while it loses 240 PgC if ECS $= 5\,^\circ$C (figure S9(j)). Under the SSP2-4.5 scenario, this range broadens to an increase of 150 PgC for ECS $= 2\,^\circ$C, and a loss of 380 PgC for ECS $= 5\,^\circ$C (figure S9(l)). SSP4-3.4 exhibits significantly smaller land carbon compared to the pre-industrial period across the entire simulated period (1850–3000 CE) (figure S9(k)), primarily due to decreasing vegetation carbon associated with higher land-use change (figure S2(d)). The land can be either a net source or sink of CO_2 emissions over the next millennium, depending on the dominant process (figures 2(a)–(c)) and S9(j)–(l)).

The positive climate–CH_4 feedback arises from the temperature dependence of the simulated natural CH_4 emissions (figures S6(a)–(c)) due to the fraction of total soil carbon respired as CH_4 from wetlands increasing with temperature. The natural CH_4 emissions are clearly dominated by tropical sources, with the extratropics playing a secondary role (figure S6).

The ocean serves as a carbon sink in all simulations (figures 2(d)–(f)) and the ocean carbon response is very similar for different ECS in our simulations (figures 2(d)–(f)). This is explained by the fact that the effect of accompanying changes in climate (positive ocean climate–carbon cycle feedback) and atmospheric CO_2 concentrations (negative ocean CO_2–carbon cycle feedback) on air-sea carbon exchange almost compensate each other. Still, the total ocean carbon uptake by 3000 CE is larger in experiments with higher ECS (figures S9(m)–(o)). While the strength of carbon cycle feedbacks depends on how different processes are represented in the model, land and ocean carbon cycle feedbacks in CLIMBER-X fall well within the range of the CMIP6 ensemble (figure 33 in Willeit *et al* 2023).

4. Discussion and conclusions

We have investigated the plausibility that the Earth system can undergo temperature changes significantly higher than usually expected in low-to-intermediate emission scenarios (SSP1-2.6, SSP2-4.5 and SSP4-3.4) under a range of ECS between $2\,^\circ$C and $5\,^\circ$C as given by the IPCC (Forster *et al* 2021). Our simulations for the three scenarios show a large spread with up to a factor >3 difference in projected global temperature change resulting from uncertainties in the ECS and its interplay with carbon cycle feedbacks. Achieving the goal of a $2\,^\circ$C increase as outlined in the Paris Agreement not only needs significant decarbonization efforts (as in SSP1-2.6 and SSP4-3.4) but also requires climate sensitivity to be $3.5\,^\circ$C or less, depending on the magnitude of carbon removal. For ECS values at the upper end, the simulated global warming generally exceeds what is typically expected for these scenarios. Global warming above $3\,^\circ$C, while unlikely, cannot be dismissed even for the present-day cumulative CO_2 emissions ($\sim$500 PgC as in SSP4-3.4, figure 1(b)). Although

SSP2-4.5 is generally perceived as a 3 °C increase scenario, we cannot exclude the possibility (i.e. with a 10% probability that ECS $>$ 4.5 °C according to Sherwood *et al* 2020) that global temperatures in this scenario could rise by more than 6 °C above pre-industrial levels (figure 1(c)). Temperature changes simulated in this case are within the range of the paleoclimate reconstructions for the middle Eocene (ca. 40 My ago), which often is referred to as a 'hothouse climate' (Burke *et al* 2018, Westerhold *et al* 2020). In previous studies, such levels of global warming were only simulated with the SSP5-8.5/RCP8.5 scenarios (Zickfeld *et al* 2013, Koven *et al* 2022), which anticipates a threefold increase in cumulative carbon emissions by 2300 CE compared to SSP2-4.5. This is explained by the combination of a broader range of ECS and explicit treatment of carbon cycle feedbacks related to both CO_2 and CH_4 in our study, which were not accounted for in the earlier investigations.

As with any study based on a single model, these results should be interpreted with recognition of inherent biases and assumptions when generalizing the effects of carbon cycle feedbacks on global warming. For example, we do not consider a potential saturation of the CO_2 fertilization effect at high CO_2 concentrations, nitrogen limitation, or extreme weather events, although these could have an impact on simulated atmospheric CO_2 concentration (Reich *et al* 2006, Frank *et al* 2015, Shi *et al* 2021). While the permafrost model used in our study is rather standard for coarse-resolution ESMs, there are indications that, in reality, permafrost degradation can occur much faster than what has been simulated (Steinert *et al* 2023). Recent studies have also shown that there is the possibility that CH_4 lifetime can increase under high anthropogenic emissions due to strong positive feedbacks (Lelieveld *et al* 1998, John *et al* 2012, Voulgarakis *et al* 2013). It is also possible that certain ocean carbon cycle processes related to the food web (Rohr *et al* 2023), ballast effect (Cram *et al* 2018), calcification (Zhang and Cao 2016), and bacteria (Kim *et al* 2023) could drive important feedbacks in the climate system, which could potentially introduce additional uncertainties. The potential contribution of methane hydrates is also not considered (Archer *et al* 2009a, Ruffine *et al* 2023). Although these unaccounted factors could potentially enhance climate–carbon cycle feedbacks, leading to increased atmospheric concentrations of CO_2 and CH_4 (and consequently, global warming), it is also possible that some of the considered positive feedbacks are overestimated in our model or that some negative feedbacks will be more significant than anticipated. This highlights the need for emissions-driven multi-model projections, especially in the framework of the forthcoming CMIP7 project (Sanderson *et al* 2024).

With high levels of global warming, as seen in all scenarios with a high ECS (figures 1(a)–(c)), it is rather likely that critical thresholds of some tipping elements of the Earth system would be breached, which could provide additional feedbacks not considered here (Winkelmann *et al* 2023, Wunderling *et al* 2024). This could have implications on sea level rise (from the Greenland and West Antarctic ice sheets), regional climate change (from the reorganization of ocean circulation, e.g. shutdown of the Atlantic Meridional Overturning Circulation), and ecosystems (from the Amazon rainforest dieback and West African monsoon shift). The impact of ocean acidification, deoxygenation, and warming, although not fully understood and only poorly accounted for in our model, could also lead to the crossing of critical thresholds with possible negative impacts on the ocean carbon sink (Heinze *et al* 2021). Although the net effect of all these changes on global climate is yet to be understood, our study demonstrates the non-negligible possibility that climate and carbon-cycle feedbacks can induce significant temperature changes, even within anthropogenic emission scenarios which are considered relatively 'safe'. This warrants careful consideration and further investigations, and emphasizes the importance of properly accounting for all major climate-related feedbacks and associated uncertainties for future climate projections.

Data availability statement

The data that support the findings of this study are openly available at the following URL/DOI: https://doi.org/10.5281/zenodo.11187708.

Acknowledgments

The authors acknowledge the pioneering work of Will Steffen, who was central in the understanding and recognition of the Anthropocene epoch. CK is funded by the Bundesgesellschaft für Endlagerung through the URS project (research Project No. STAFuE-21-4-Klei). MW is funded by the German climate modeling project PalMod supported by the German Federal Ministry of Education and Research (BMBF) as a Research for Sustainability initiative (FONA) (Grant Nos. 01LP1920B, 01LP1917D, 01LP2305B). ST is supported by the European Research Council (Project Earth Resilience in the Anthropocene, ERC-2016-ADG 743080); European Research Council (ERC) under the European Union's Horizon 2020 research and innovation programme (Grant No. 819202). The authors gratefully acknowledge the European Regional Development Fund (ERDF), the German Federal Ministry of Education and Research, and the Land Brandenburg for supporting this project by providing resources on the high-performance computer system at the Potsdam Institute for Climate Impact Research.

Conflict of interest

The authors declare no competing interests.

ORCID iDs

Christine Kaufhold https://orcid.org/0009-0001-1772-9039
Matteo Willeit https://orcid.org/0000-0003-3998-6404
Stefanie Talento https://orcid.org/0000-0003-0100-5033
Johan Rockström https://orcid.org/0000-0001-8988-2983

References

Archer D and Brovkin V 2008 The millennial atmospheric lifetime of anthropogenic CO_2 *Clim. Change* **90** 283–97
Archer D, Buffett B and Brovkin V 2009a Ocean methane hydrates as a slow tipping point in the global carbon cycle *Proc. Natl Acad. Sci.* **106** 20596–601
Archer D *et al* 2009b Atmospheric lifetime of fossil fuel carbon dioxide *Annu. Rev. Earth Planet. Sci.* **37** 117–34
Arora V K *et al* 2020 Carbon–concentration and carbon–climate feedbacks in CMIP6 models and their comparison to CMIP5 models *Biogeosciences* **17** 4173–222
Asaadi A, Schwinger J, Lee H, Tjiputra J, Arora V, Séférian R, Liddicoat S, Hajima T, Santana-Falcón Y and Jones C D 2024 Carbon cycle feedbacks in an idealized simulation and a scenario simulation of negative emissions in CMIP6 Earth system models *Biogeosciences* **21** 411–35
Bjordal J, Storelvmo T, Alterskjær K and Carlsen T 2020 Equilibrium climate sensitivity above 5 °C plausible due to state-dependent cloud feedback *Nat. Geosci.* **13** 718–21
Bloch-Johnson J, Rugenstein M, Stolpe M B, Rohrschneider T, Zheng Y and Gregory J M 2021 Climate sensitivity increases under higher CO_2 levels due to feedback temperature dependence *Geophys. Res. Lett.* **48** e2020GL089074
Booth B B B, Harris G R, Murphy J M, House J I, Jones C D, Sexton D and Sitch S 2017 Narrowing the range of future climate projections using historical observations of atmospheric CO_2 *J. Clim.* **30** 3039–53
Bouttes N, Kwiatkowski L, Bougeot E, Berger M, Brovkin V and Munhoven G 2024 Projections of coral reef carbonate production from a global climate-coral reef coupled model *EGUsphere* **2024** 1–25
Brovkin V *et al* 2013 Effect of anthropogenic land-use and land-cover changes on climate and land carbon storage in CMIP5 projections for the twenty-first century *J. Clim.* **26** 6859–81
Burgess M G, Ritchie J, Shapland J and Pielke R 2020 IPCC baseline scenarios have over-projected CO_2 emissions and economic growth *Environ. Res. Lett.* **16** 014016
Burke K D, Williams J W, Chandler M A, Haywood A M, Lunt D J and Otto-Bliesner B L 2018 Pliocene and Eocene provide best analogs for near-future climates *Proc. Natl Acad. Sci.* **115** 13288–93
Caballero R and Huber M 2013 State-dependent climate sensitivity in past warm climates and its implications for future climate projections *Proc. Natl Acad. Sci.* **110** 14162–7
Caldwell P M, Zelinka M D and Klein S A 2018 Evaluating emergent constraints on equilibrium climate sensitivity *J. Clim.* **31** 3921–42
Carslaw K S *et al* 2013 Large contribution of natural aerosols to uncertainty in indirect forcing *Nature* **503** 67–71
Clark P U *et al* 2016 Consequences of twenty-first-century policy for multi-millennial climate and sea-level change *Nat. Clim. Change* **6** 360–9
Colbourn G, Ridgwell A and Lenton T M 2015 The time scale of the silicate weathering negative feedback on atmospheric CO_2 *Glob. Biogeochem. Cycles* **29** 583–96
Cram J A, Weber T, Leung S W, McDonnell A M P, Liang J-H and Deutsch C 2018 The role of particle size, ballast, temperature and oxygen in the sinking flux to the deep sea *Glob. Biogeochem. Cycles* **32** 858–76
Davidson J P L and Kemp L 2024 Climate catastrophe: the value of envisioning the worst-case scenarios of climate change *Wiley Interdiscip. Rev. Clim. Change* **15** e871
Flynn C M and Mauritsen T 2020 On the climate sensitivity and historical warming evolution in recent coupled model ensembles *Atmos. Chem. Phys.* **20** 7829–42
Forster P *et al* 2021 Chapter 7: The Earth's energy budget, climate feedbacks and climate sensitivity *Climate Change 2021: The Physical Science Basis. Contribution of Working Group I to the Sixth Assessment Report of the Intergovernmental Panel on Climate Change* ed V Masson-Delmotte *et al* (Cambridge University Press) book section 7
Frank D *et al* 2015 Effects of climate extremes on the terrestrial carbon cycle: concepts, processes and potential future impacts *Glob. Change Biol.* **21** 2861–80
Friedlingstein P *et al* 2023 Global carbon budget 2023 *Earth Syst. Sci. Data* **15** 5301–69
Ganopolski A, Winkelmann R and Schellnhuber H J 2016 Critical insolation-CO_2 relation for diagnosing past and future glacial inception *Nature* **534** 200–3
Gillett N P, Arora V K, Zickfeld K, Marshall S J and Merryfield W J 2011 Ongoing climate change following a complete cessation of carbon dioxide emissions *Nat. Geosci.* **4** 83–7
Govindasamy B, Thompson S, Mirin A, Wickett M, Caldeira K and Delire C 2005 Increase of carbon cycle feedback with climate sensitivity: results from a coupled climate and carbon cycle model *Tellus* B **57** 153–63
Gregory J M, Andrews T, Ceppi P, Mauritsen T and Webb M J 2020 How accurately can the climate sensitivity to CO_2 be estimated from historical climate change? *Clim. Dyn.* **54** 129–57
Hausfather Z 2025 An assessment of current policy scenarios over the 21st century and the reduced plausibility of high-emissions pathways *Dialogues Clim. Change* **1** 29768659241304854
Hausfather Z and Peters G P 2020 Emissions—the 'business as usual' story is misleading *Nature* **577** 618–20
Heinze C *et al* 2021 The quiet crossing of ocean tipping points *Proc. Natl Acad. Sci.* **118** e2008478118
Hermans T H J, Gregory J M, Palmer M D, Ringer M A, Katsman C A and Slangen A B A 2021 Projecting global mean sea-level change using CMIP6 models *Geophys. Res. Lett.* **48** e2020GL092064
Huusko L, Bender F A-M, Ekman A M L and Storelvmo T 2021 Climate sensitivity indices and their relation with projected temperature change in CMIP6 models *Environ. Res. Lett.* **16** 064095
International Energy Agency 2023 Coal 2023: analysis and forecast to 2026 *Technical Report* (International Energy Agency) (available at: www.iea.org/reports/coal-2023)
John J G, Fiore A M, Naik V, Horowitz L W and Dunne J P 2012 Climate versus emission drivers of methane lifetime against loss by tropospheric OH from 1860–2100 *Atmos. Chem. Phys.* **12** 12021–36
Kemp L *et al* 2022 Climate endgame: exploring catastrophic climate change scenarios *Proc. Natl Acad. Sci.* **119** e2108146119
Kim H H, Laufkötter C, Lovato T, Doney S C and Ducklow H W 2023 Projected 21st-century changes in marine heterotrophic bacteria under climate change *Front. Microbiol.* **14** 1049579

Kleinen T, Gromov S, Steil B and Brovkin V 2021 Atmospheric methane underestimated in future climate projections *Environ. Res. Lett.* **16** 094006
Knutti R, Rugenstein M A A and Hegerl G C 2017 Beyond equilibrium climate sensitivity *Nat. Geosci.* **10** 727–36
Köhler P, Nehrbass-Ahles C, Schmitt J, Stocker T F and Fischer H 2017 A 156 kyr smoothed history of the atmospheric greenhouse gases CO_2, CH_4 and N_2O and their radiative forcing *Earth Syst. Sci. Data* **9** 363–87
Koven C D *et al* 2022 Multi-century dynamics of the climate and carbon cycle under both high and net negative emissions scenarios *Earth Syst. Dyn.* **13** 885–909
Lee L A, Reddington C L and Carslaw K S 2016 On the relationship between aerosol model uncertainty and radiative forcing uncertainty *Proc. Natl Acad. Sci.* **113** 5820–7
Lelieveld J, Crutzen P J and Dentener F J 1998 Changing concentration, lifetime and climate forcing of atmospheric methane *Tellus* B **50** 128–50
Lohmann U, Rotstayn L, Storelvmo T, Jones A, Menon S, Quaas J, Ekman A M L, Koch D and Ruedy R 2010 Total aerosol effect: radiative forcing or radiative flux perturbation? *Atmos. Chem. Phys.* **10** 3235–46
MacDougall A H *et al* 2020 Is there warming in the pipeline? A multi-model analysis of the zero emissions commitment from CO_2 *Biogeosciences* **17** 2987–3016
Mann M E 2021 Beyond the hockey stick: climate lessons from the common era *Proc. Natl Acad. Sci.* **118** e2112797118
Meehl G A, Senior C A, Eyring V, Flato G, Lamarque J-F, Stouffer R J, Taylor K E and Schlund M 2020 Context for interpreting equilibrium climate sensitivity and transient climate response from the CMIP6 Earth system models *Sci. Adv.* **6** 1–11
Meinshausen M *et al* 2020 The Shared Socio-economic pathway (SSP) greenhouse gas concentrations and their extensions to 2500 *Geosci. Model Dev.* **13** 3571–605
Melnikova I, Boucher O, Cadule P, Ciais P, Gasser T, Quilcaille Y, Shiogama H, Tachiiri K, Yokohata T and Tanaka K 2021 Carbon cycle response to temperature overshoot beyond 2 °C: an analysis of CMIP6 models *Earth's Future* **9** e2020EF001967
Mikolajewicz U, Gröger M, Maier-Reimer E, Schurgers G, Vizcaíno M and Winguth A M E 2007 Long-term effects of anthropogenic CO_2 emissions simulated with a complex Earth system model *Clim. Dyn.* **28** 599–633
Morice C P, Kennedy J J, Rayner N A, Winn J P, Hogan E, Killick R E, Dunn R J H, Osborn T J, Jones P D and Simpson I R 2021 An updated assessment of near-surface temperature change from 1850: the HadCRUT5 data set *J. Geophys. Res. Atmos.* **126** e2019JD032361
Murphy J M, Sexton D M H, Barnett D N, Jones G S, Webb M J, Collins M and Stainforth D A 2004 Quantification of modelling uncertainties in a large ensemble of climate change simulations *Nature* **430** 768–72
Myhre G, Myhre C E L, Samset B H and Storelvmo T 2013 Aerosols and their relation to global climate and climate sensitivity *Nat. Educ. Knowl.* **4** 7
Nijsse F J M M, Cox P M and Williamson M S 2020 Emergent constraints on transient climate response (TCR) and equilibrium climate sensitivity (ECS) from historical warming in CMIP5 and CMIP6 models *Earth Syst. Dyn.* **11** 737–50
Pfister P L and Stocker T F 2017 State-dependence of the climate sensitivity in Earth system models of intermediate complexity *Geophys. Res. Lett.* **44** 10643–53
Pielke Jr R, Burgess M G and Ritchie J 2022 Plausible 2005–2050 emissions scenarios project between 2 °C and 3 °C of warming by 2100 *Environ. Res. Lett.* **17** 024027
Reich P B, Hobbie S E, Lee T, Ellsworth D S, West J B, Tilman D, Knops J M H, Naeem S and Trost J 2006 Nitrogen limitation constrains sustainability of ecosystem response to CO_2 *Nature* **440** 922–5
Rohling E J *et al* (PALAEOSENS Project Members) 2012 Making sense of palaeoclimate sensitivity *Nature* **491** 683–91
Rohr T, Richardson A J, Lenton A, Chamberlain M A and Shadwick E H 2023 Zooplankton grazing is the largest source of uncertainty for marine carbon cycling in CMIP6 models *Commun. Earth Environ.* **4** 212
Ruffine L, Tang A M, O'Neill N, Toffin L, Paris J-D, Yang J, Georgiev V, Fietzek P, Giustiniani M and Tinivella U 2023 Environmental challenges related to methane hydrate decomposition from climate change scenario and anthropic activities: state of the art, potential consequences and monitoring solutions *Earth-Sci. Rev.* **246** 104578
Rugenstein M *et al* 2020 Equilibrium climate sensitivity estimated by equilibrating climate models *Geophys. Res. Lett.* **47** e2019GL083898
Sanderson B M *et al* 2024 The need for carbon-emissions-driven climate projections in CMIP7 *Geosci. Model Dev.* **17** 8141–72
Schneider T, Kaul C M and Pressel K G 2019 Possible climate transitions from breakup of stratocumulus decks under greenhouse warming *Nat. Geosci.* **12** 163–7
Schneider von Deimling T, Held H, Ganopolski A and Rahmstorf S 2006 Climate sensitivity estimated from ensemble simulations of glacial climate *Clim. Dyn.* **27** 149–63
Shaffer G, Huber M, Rondanelli R and Pedersen J O P 2016 Deep time evidence for climate sensitivity increase with warming *Geophys. Res. Lett.* **43** 6538–45
Sherwood S C and Forest C E 2024 Opinion: can uncertainty in climate sensitivity be narrowed further? *Atmos. Chem. Phys.* **24** 2679–86
Sherwood S C *et al* 2020 An assessment of Earth's climate sensitivity using multiple lines of evidence *Rev. Geophys.* **58** e2019RG000678
Shi H *et al* 2021 Saturation of global terrestrial carbon sink under a high warming scenario *Glob. Biogeochem. Cycles* **35** e2020GB006800
Solomon S, Plattner G-K, Knutti R and Friedlingstein P 2009 Irreversible climate change due to carbon dioxide emissions *Proc. Natl Acad. Sci.* **106** 1704–9
Steffen W *et al* 2018 Trajectories of the Earth system in the Anthropocene *Proc. Natl Acad. Sci.* **115** 8252–9
Steinert N J, Debolskiy M V, Burke E J, García-Pereira F and Lee H 2023 Evaluating permafrost definitions for global permafrost area estimates in CMIP6 climate models *Environ. Res. Lett.* **19** 014033
Tanaka K and O'Neill B C 2018 The Paris Agreement zero-emissions goal is not always consistent with the 1.5 °C and 2 °C temperature targets *Nat. Clim. Change* **8** 319–24
Tokarska K B, Stolpe M B, Sippel S, Fischer E M, Smith C J, Lehner F and Knutti R 2020 Past warming trend constrains future warming in CMIP6 models *Sci. Adv.* **6** 1–14
UNFCC 2015 The Paris Agreement (available at: https://unfccc.int/process-and-meetings/the-paris-agreement)
Voulgarakis A *et al* 2013 Analysis of present day and future OH and methane lifetime in the ACCMIP simulations *Atmos. Chem. Phys.* **13** 2563–87
Wall C J, Norris J R, Possner A, McCoy D T, McCoy I L and Lutsko N J 2022 Assessing effective radiative forcing from aerosol–cloud interactions over the global ocean *Proc. Natl Acad. Sci.* **119** e2210481119
Westerhold T *et al* 2020 An astronomically dated record of Earth's climate and its predictability over the last 66 million years *Science* **369** 1383–7
Willeit M, Calov R, Talento S, Greve R, Bernales J, Klemann V, Bagge M and Ganopolski A 2024 Glacial inception through rapid ice area increase driven by albedo and vegetation feedbacks *Clim. Past* **20** 597–623
Willeit M, Ganopolski A, Robinson A and Edwards N R 2022 The Earth system model CLIMBER-X v1.0—part 1: climate model description and validation *Geosci. Model Dev.* **15** 5905–48

Willeit M *et al* 2023 The Earth system model CLIMBER-X v1.0—part 2: the global carbon cycle *Geosci. Model Dev.* **16** 3501–34

Winkelmann R *et al* 2023 Chapter 1.2: Tipping points in the cryosphere *Global Tipping Points Report 2023* ed J Dearing, C Folke, M T Huber, C Koven, C Muller, T Naish, S Rahmstorf, A K Seshadri and S Willcock (University of Exeter) book section 1.2

Wunderling N *et al* 2024 Climate tipping point interactions and cascades: a review *Earth Syst. Dyn.* **15** 41–74

Yamazaki K, Sexton D M H, Rostron J W, McSweeney C F, Murphy J M and Harris G R 2021 A perturbed parameter ensemble of HadGEM3-GC3.05 coupled model projections: part 2: global performance and future changes *Clim. Dyn.* **56** 3437–71

Zelinka M D, Klein S A, Taylor K E, Andrews T, Webb M J, Gregory J M and Forster P M 2013 Contributions of different cloud types to feedbacks and rapid adjustments in CMIP5 *J. Clim.* **26** 5007–27

Zelinka M D, Myers T A, McCoy D T, Po-Chedley S, Caldwell P M, Ceppi P, Klein S A and Taylor K E 2020 Causes of higher climate sensitivity in CMIP6 models *Geophys. Res. Lett.* **47** e2019GL085782

Zhang H and Cao L 2016 Simulated effect of calcification feedback on atmospheric CO_2 and ocean acidification *Sci. Rep.* **6** 20284

Zickfeld K *et al* 2013 Long-term climate change commitment and reversibility: an EMIC intercomparison *J. Clim.* **26** 5782–809